Check for updates

The COP1 Target SHI-RELATED SEQUENCE5 Directly Activates Photomorphogenesis-Promoting Genes

Ting-Ting Yuan, Heng-Hao Xu, Qing Zhang, Lin-Yu Zhang, and Ying-Tang Lu[1]

State Key Laboratory of Hybrid Rice, College of Life Sciences, Wuhan University, Wuhan 430072, China

ORCID IDs: 0000-0002-8577-3584 (T.-T.Y.); 0000-0003-1701-3484 (H.-H.X.); 0000-0002-7921-2991 (Q.Z.); 0000-0002-7947-4086 (L.-Y.Z.); 0000-0003-3540-6935 (Y.-T.L.)

Plant seedlings undergo distinct developmental processes in the dark and in the light. Several genes, including *ELONGATED HYPOCOTYL5* (*HY5*), *B-BOX PROTEIN21* (*BBX21*), and *BBX22*, have been identified as photomorphogenesis-promoting factors in *Arabidopsis thaliana*; however, the overexpression of these genes does not induce photomorphogenesis in the dark. Using an activation-tagging approach, we identified *SRS5ox*, which overexpresses *SHI-RELATED SEQUENCE5* (*SRS5*) following induction with estradiol. *SRS5* overexpression in *SRS5ox* and *Pro35S:SRS5-GFP* seedlings results in a constitutive photomorphogenesis phenotype in the dark, whereas *SRS5* loss of function in the *srs5-2* mutant results in long hypocotyls in the light. This indicates that SRS5 is a positive regulator of photomorphogenesis. Furthermore, SRS5 promotes photomorphogenesis by directly binding to the promoters of photomorphogenesis-promoting genes, such as *HY5*, *BBX21*, and *BBX22*, and activating their expression, thus affecting the expression of downstream light-signaling genes. These data indicate that SRS5 acts in the upregulation of photomorphogenesis-promoting genes. In addition, CONSTITUTIVELY PHOTOMORPHOGENIC1 (COP1), which plays a central repressive role in seedling photomorphogenesis, directly ubiquitinates SRS5, promoting its degradation in the dark. Taken together, our results demonstrate that SRS5 directly activates the expression of downstream genes *HY5*, *BBX21*, and *BBX22* and is a target of COP1-mediated degradation in Arabidopsis.

INTRODUCTION

In addition to providing biological energy via photosynthesis, light is an informative environmental signal that influences growth and development in plants (Chen et al., 2004; Kami et al., 2010). In the light, seedlings undergo photomorphogenesis, having compact hypocotyls and open cotyledons with mature chloroplasts. By contrast, seedlings grown in the dark undergo skotomorphogenesis, having etiolated hypocotyls and developing etioplasts in closed cotyledons protected by the apical hook.

Plants perceive light via intracellular photoreceptors, which govern molecular signaling pathways that ultimately modulate the transcriptome and cause changes in growth and development. Microarray analysis has revealed that up to a third of *Arabidopsis thaliana* genes exhibit altered expression in seedlings grown in the dark, compared with those grown in the light (Ma et al., 2001). One such gene is *ELONGATED HYPOCOTYL5* (*HY5*), which is a positive regulator of light-regulated processes, based on the partially etiolated phenotype of light-grown *hy5* seedlings; HY5 also plays a key signaling role in the developmental transition from dark to light (Osterlund et al., 2000b; Lee et al., 2007; Zhang et al., 2011). In the light, *HY5* expression increases and the resulting increased abundance of HY5 facilitates the expression of a large number of photomorphogenesis-promoting genes (Osterlund et al., 2000a; Lee et al., 2007; Zhang et al., 2011).

Multiple factors regulate *HY5* expression and HY5 protein levels. For example, CALMODULIN7, a unique member of the calmodulin family, functions as a transcription regulator to modulate *HY5* expression by directly binding to the *HY5* promoter besides its interaction with HY5 (Abbas et al., 2014). In addition, HY5 and its homolog HYH also bind to the *HY5* promoter to activate *HY5* transcription in response to UV-B (Binkert et al., 2014). Recent work showed that the transcription factor B-BOX PROTEIN21 (BBX21) can bind the T/G box in the *HY5* promoter and thus was also implicated in *HY5* transcriptional regulation (Xu et al., 2016). In the dark, skotomorphogenesis is promoted through HY5 ubiquitination by the E3 ubiquitin ligase CONSTITUTIVELY PHOTOMORPHOGENIC1 (COP1), which leads to HY5 degradation via the 26S proteasome (Lau and Deng, 2012; Huang et al., 2014). Thus, COP1 activity directly affects seedling photomorphogenesis (Lau and Deng, 2012; Huang et al., 2014).

COP1 functions as a central repressor of seedling photomorphogenesis and *cop1* mutant seedlings that produce an impaired version of COP1 exhibit constitutive photomorphogenesis when grown in the dark (Lau and Deng, 2010). In wild-type seedlings grown in the dark, nuclear-localized COP1 ubiquitinates HY5, promoting its degradation (Osterlund et al., 2000b; Wang et al., 2001; Lau and Deng, 2010), whereas light exposure reduces nuclear COP1 to a level that permits the accumulation of HY5 (von Arnim and Deng, 1994; von Arnim et al., 1997). Light also represses COP1 activity by activating the photoreceptors phytochrome A (phyA) and phyA/B and cryptochrome 1 (CRY1) and CRY2 to modulate the complex between COP1 and SUPPRESSOR OF PHYA-105, ultimately leading to HY5 accumulation (Yang et al., 2000, 2001; Hoecker and Quail, 2001; Wang et al., 2001; Saijo et al., 2003; Sang et al., 2005).

HY5 was the first protein shown to be regulated by COP1; however, HY5 does not act alone in the promotion of light responses (Ang et al., 1998; Datta et al., 2008; Chang et al., 2011). Subsequent studies have revealed that a series of B-box-containing proteins, including BBX21 and BBX22, are also direct targets of COP1 (Datta et al., 2008; Chang et al., 2011). BBX-containing proteins share many roles with HY5 in response to light, such as the regulation of anthocyanin accumulation and the inhibition of seedling hypocotyl elongation (Holm et al., 2002; Datta et al., 2008; Chang et al., 2011; Binkert et al., 2014; Xu et al., 2016). It is also known that BBX22 can interact with HY5 and that BBX21 modulates *HY5* expression though its binding to the promoter of *HY5* (Holm et al., 2002; Datta et al., 2008; Chang et al., 2011; Binkert et al., 2014; Xu et al., 2016). However, no corresponding overexpression lines (*35S:HY5*, *35S:BBX21*, and *35S:BBX22*) exhibit constitutive photomorphogenesis comparable to *cop1* seedlings in the dark (Ang et al., 1998; Holm et al., 2002; Chang et al., 2011; Xu et al., 2016). Furthermore, it remains unclear whether and how additional unidentified regulator(s) play a role in photomorphogenesis.

In this study, we describe the identification and characterization of SRS5 as a positive regulator of photomorphogenesis. *SRS5* belongs to *SHORT-INTERNODES* (*SHI*) gene family, members of which act as transcription factors involved in regulating the development of diverse plant organs (Fridborg et al., 1999; Kuusk et al., 2002; Baylis et al., 2013). We demonstrate that *SRS5* overexpression seedlings exhibit photomorphogenesis in the dark, whereas light-grown seedlings of the *srs5-2* mutant line display greater hypocotyl elongation compared with wild-type seedlings. Furthermore, light-induced *SRS5* accumulation promotes seedling photomorphogenesis via direct activation of a number of other photomorphogenesis-promoting genes such as *HY5*, *BBX21*, and *BBX22*. In the dark, SRS5 is targeted by COP1 for 26S proteasome-mediated degradation.

RESULTS

SRS5 Functions as a Positive Regulator of Photomorphogenesis

To investigate the regulatory mechanisms behind photomorphogenesis, we employed a chemically inducible activation tagging approach to identify genes that play a role in this process, in particular to identify those genes with redundant functions or lethal mutant phenotypes (Marsch-Martínez and Pereira, 2011). Arabidopsis T-DNA insertion lines generated with an estradiol-inducible expression system driven by the chimeric transcription activator XVE (Zuo et al., 2000) were screened for photomorphogenesis in the dark in the presence of estradiol. This led to the isolation of a mutant line displaying short hypocotyls and open cotyledons, which we designated *SRS5ox* based on our subsequent characterization (Figure 1A).

To characterize the genomic sequence flanking the XVE T-DNA in *SRS5ox*, we performed thermal asymmetric interlaced PCR. This identified the T-DNA insertion site as 2528 bp upstream of the predicted translation start site of *SRS5* (Figure 1B), a *SHI* family gene encoding a protein with a RING finger-like zinc finger motif (Kuusk et al., 2006). Subsequent reverse transcription-quantitative PCR (RT-qPCR) analyses revealed that *SRS5* expression was significantly induced in estradiol-treated *SRS5ox* seedlings (Figure 1C).

To further examine the *SRS5ox* phenotype, wild-type and *SRS5ox* seedlings were grown on medium with or without estradiol in the dark for 5 d. Whereas wild-type seedlings displayed skotomorphogenesis under these conditions, *SRS5ox* seedlings displayed photomorphogenesis with shorter hypocotyls and open cotyledons (Figures 1D and 1E). Furthermore, seedlings expressing *SRS5-GFP* driven by the cauliflower mosaic virus 35S promoter (*Pro35S:SRS5-GFP*) also exhibited shorter hypocotyls when grown in the dark, compared with the wild-type seedlings; however, these transgenic seedlings maintained closed cotyledons in the dark, which may be attributed to a lower *SRS5* expression level compared with that in *SRS5ox* (Figures 1C to 1E). Combined, these results indicate that *SRS5* overexpression leads to photomorphogenesis in the dark.

Following this, we examined light responsiveness in *SRS5ox* seedlings and observed that, compared with the wild type, the hypocotyls of estradiol-treated *SRS5ox* seedlings were significantly shorter when grown in various fluence rates of different light (Figures 1D to 1F; Supplemental Figure 1). In agreement, seedlings of the loss-of-function homozygous mutant *srs5-2* (Salk_019951) had hypocotyls that were longer than wild-type hypocotyls when grown in various fluence rates of different light, though hypocotyl length was comparable between *srs5-2* and wild-type seedlings grown in the dark (Figures 1D to 1F; Supplemental Figure 1). Moreover, the *Pro35S:SRS5-GFP* transgenic lines displayed shorter hypocotyls when grown in the different light conditions, compared with the wild-type seedlings. The *srs5-2* mutant phenotype was rescued by *SRS5* overexpression, as demonstrated by the comparable hypocotyl elongation in *srs5-2 Pro35S:SRS5-GFP* and *Pro35S:SRS5-GFP* seedlings grown either in the different light conditions or in the dark (Figures 1D and 1E; Supplemental Figures 1A and 1B). Collectively, our data indicate that *SRS5* functions as a positive regulator of photomorphogenesis.

Blue Light Promotes *SRS5* Expression

We examined whether *SRS5* is regulated by blue light by conducting a time-course analysis of *SRS5* expression. For this purpose, 5-d-old Arabidopsis seedlings grown in the dark were treated with blue, red, or far-red light for 0, 3, 6, or 12 h, and *SRS5* expression was measured by RT-qPCR. We observed a significant increase in *SRS5* expression following blue light exposure (Figure 2A). Then, we examined the *SRS5* expression in *cry1* and *cry1 cry2* mutants. Our results showed that blue light-induced accumulation of *SRS5* transcripts was repressed in the mutants (Figure 2C). Consistently, higher SRS5 protein accumulation by blue light was also reduced in the mutants (Figure 2D). However, while our phenotype analysis showed that *SRS5* was needed for photomorphogenesis under red and far-red light (Supplemental Figure 1), similar levels of *SRS5* transcript were detected after treating with red or far-red light compared with dark-treated control (Supplemental Figure 2).
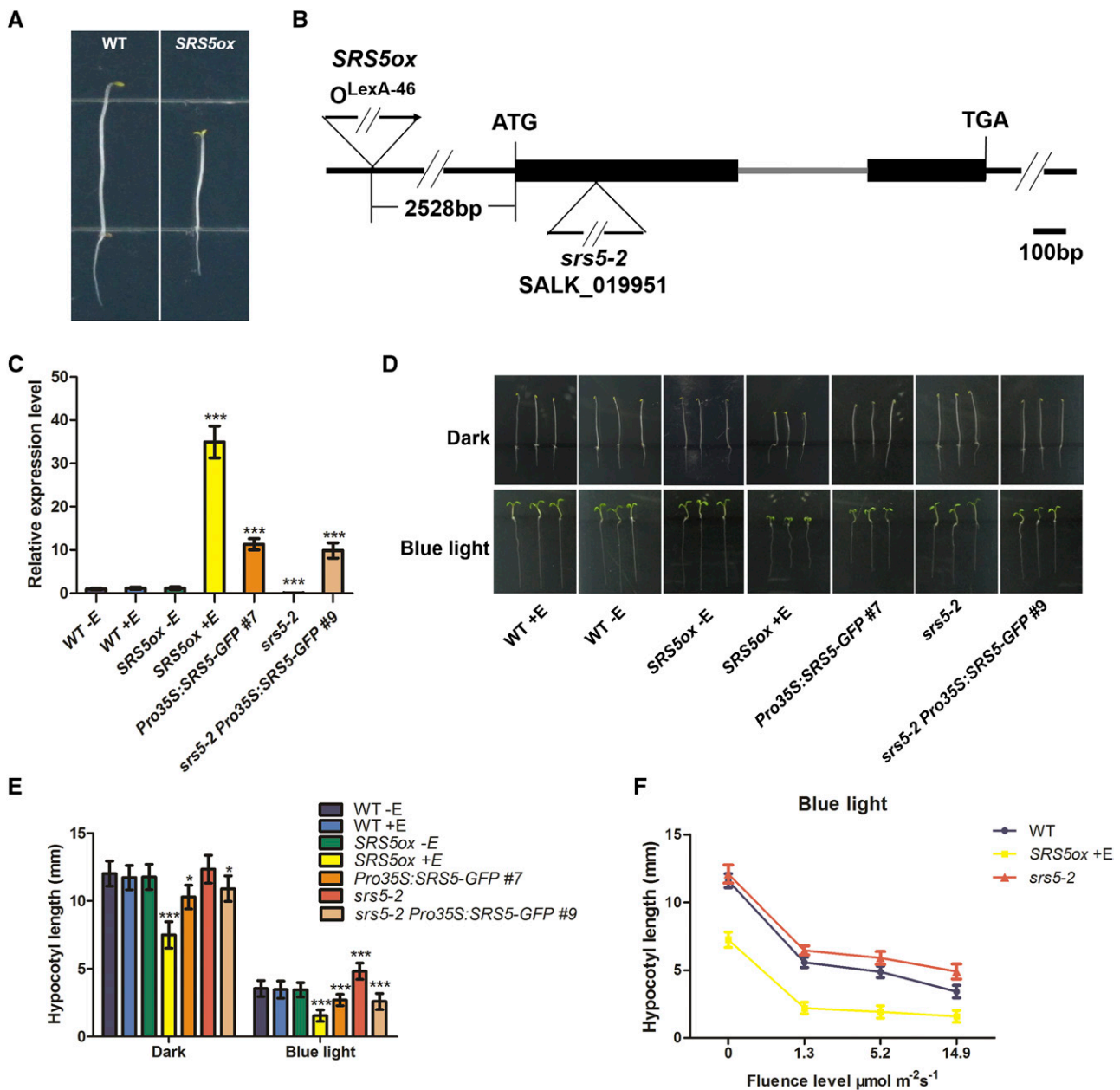
Figure 1. Phenotypes of *SRS5ox* and *srs5-2* Seedlings.

(A) Photographs show the dark-grown phenotypes of wild-type seedlings and *SRS5ox* seedlings treated with 5 μM estradiol.

(B) Schematic representation of the T-DNA insertion sites in *SRS5* (At1g75520) in the *SRS5ox* and *srs5-2* mutant lines. Black boxes represent exons, the gray line represents an intron, and the black lines represent regions upstream and downstream of the gene.

(C) *SRS5* expression level assayed by RT-qPCR in seedlings of the wild type (± estradiol treatment), *SRS5ox* (± estradiol treatment), *Pro35S:SRS5-GFP*, *srs5-2*, and *srs5-2 Pro35S:SRS5-GFP*. *SRS5* expression in all lines was normalized to that in nontreated wild-type seedlings, which was set to 1. Data are means ± SD of three independent biological replicates. Asterisks indicate significant difference at ***$P < 0.001$ (Student's *t* test; Supplemental File 1).

(D) Phenotypes of 5-d-old seedlings grown with (+E) or without (−E) 5 μM estradiol in the dark or in blue light (14.9 μmol m^{-2} s^{-1}). Bar = 5 mm.

(E) Hypocotyl lengths of 5-d-old seedlings grown with (+E) or without (−E) 5 μM estradiol in the dark or in blue light (14.9 μmol m^{-2} s^{-1}). Data are means ± SD; $n \geq 30$. Asterisks indicate significant differences with respect to each control (Student's *t* test): *$P < 0.05$ and ***$P < 0.001$. Data are shown from *Pro35S:SRS5-GFP* line #7 and *srs5-2 Pro35S:SRS5-GFP* line #9, which are representative of three independent transgenic lines for each genotype.

(F) Hypocotyl lengths of wild-type, *srs5-2*, and estradiol-treated *SRS5ox* seedlings grown under various fluence rates of blue light. Data are means ± SD; $n \geq 30$.
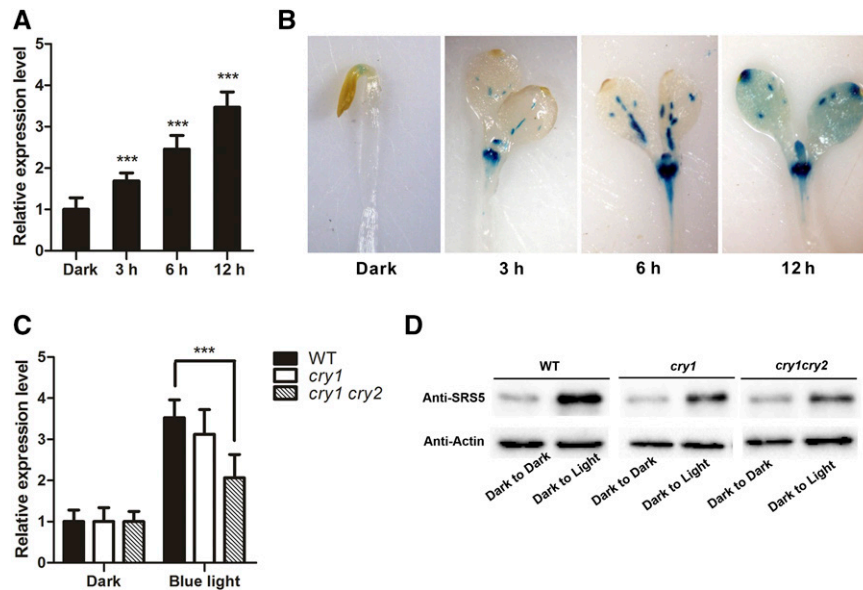
Figure 2. *SRS5* Expression Is Significantly Induced by Blue Light.

(A) The *SRS5* expression level as measured by RT-qPCR in 5-d-old wild-type seedlings grown in the dark and treated with blue light (14.9 μmol m^{-2} s^{-1}) for either 0, 3, 6, or 12 h. Expression levels were normalized against that in continuous dark-treated seedlings, which was set to 1. Data are means ± SD of three independent biological replicates. Asterisks indicate significant difference at ***P < 0.001 (Student's *t* test; Supplemental File 1).
(B) GUS staining in 5-d-old *ProSRS5:GUS* transgenic seedlings treated with blue light for either 0, 3, 6, or 12 h.
(C) *SRS5* expression as measured by RT-qPCR in 5-d-old wild-type, *cry1*, and *cry1 cry2* seedlings grown in the dark and treated with blue light (14.9 μmol m^{-2} s^{-1}) for 12 h. Expression levels were normalized against that in continuous dark-treated wild-type seedlings, which was set to 1. Data are means ± SD of three independent biological replicates. Asterisks indicate significant difference at ***P < 0.001 (Student's *t* test).
(D) Immunodetection of SRS5 in 5-d-old wild-type, *cry1*, and *cry1 cry2* seedlings grown in the dark and treated with blue light (14.9 μmol m^{-2} s^{-1}) for 12 h. Anti-actin served as a loading control.

To verify this result, we generated *ProSRS5:GUS* transgenic plants and monitored *SRS5* expression via GUS staining of dark-grown *ProSRS5:GUS* seedlings following blue light treatment for 0, 3, 6, or 12 h. This revealed *SRS5* expression in dark-grown etiolated seedlings in the apical hook, whereas *SRS5* expression was significantly induced in the cotyledons and hypocotyl following blue light treatment (Figure 2B).

Therefore, in combination with the role of SRS5 in blue light-dependent photomorphogenesis described above, these data suggest that blue light modulates photomorphogenesis by stimulating *SRS5* expression.

SRS5 Promotes Photomorphogenesis by Directly Activating *HY5* Expression

HY5, a positive regulator of photomorphogenesis, is also induced by blue light (Osterlund et al., 2000b; Lee et al., 2007; Zhang et al., 2011). Therefore, to investigate the potential crosstalk between HY5 and SRS5, we analyzed *HY5* expression in *srs5-2* and estradiol-treated *SRS5ox*. More *HY5* transcript accumulated in estradiol-treated *SRS5ox* seedlings than in the wild type, whereas *HY5* expression was lower in *srs5-2* seedlings than in wild-type seedlings, which suggests that the function of SRS5 in photomorphogenesis involves induction of *HY5* expression (Figure 3A). This hypothesis was further supported

by the significant increase in HY5 abundance observed in estradiol-treated *SRS5ox* seedlings, which was attributed to *SRS5* overexpression, and the decreased HY5 abundance in *srs5-2* mutants (Figure 3B).

Like STYLISH1 (STY1), another SHI family member that is present in the nucleus (Eklund et al., 2010), SRS5 was also found to be nuclear localized (Figure 3C), suggesting that SRS5 may act as a transcription factor to promote *HY5* expression. Therefore, we examined whether SRS5 associates with the *HY5* promoter region via chromatin immunoprecipitation (ChIP) assays using anti-SRS5 antibody prepared with SRS5 purified from *Escherichia coli* (Supplemental Figure 3). We found that the P1 region of the *HY5* promoter was strongly enriched among the immunoprecipitated chromatin of estradiol-treated *SRS5ox* plants compared with that of nontreated *SRS5ox* plants (Figures 3D and 3E), suggesting that SRS5 binds to this *HY5* promoter region.

To verify this result, we conducted DNA electrophoretic mobility shift assays (EMSAs) using SRS5 purified as described above. SRS5 bound to the DNA probe corresponding to the P1 region, and an unlabeled version of this DNA probe (competitor) could compete for SRS5 binding (Figure 3F). Analysis of the DNA probe revealed the nucleotides ACTCTAC (−742 to −735 bp) in the antisense sequence corresponding to the STY1 binding site consensus sequence (Eklund et al., 2010), which suggests that
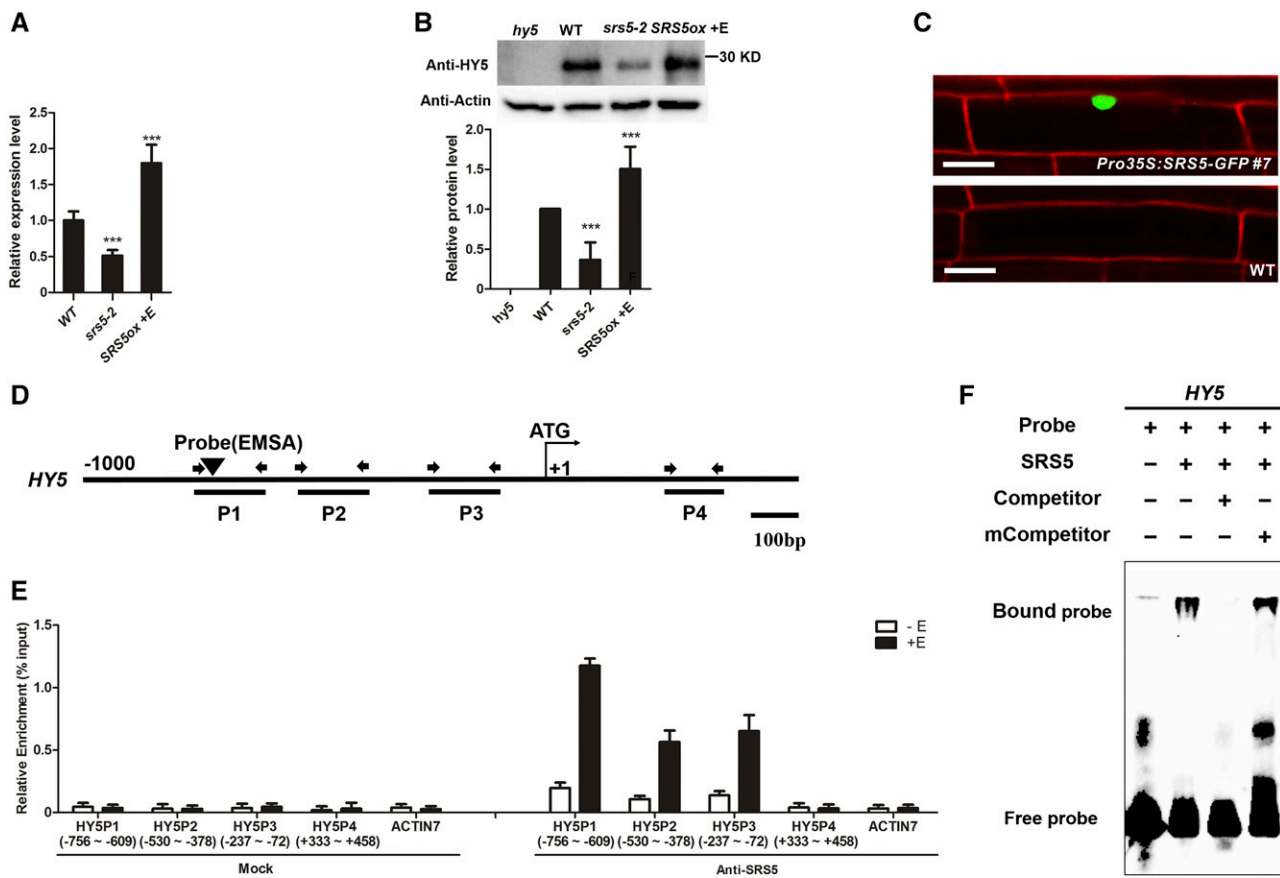
Figure 3. SRS5 Activates *HY5* Expression by Directly Binding to Its Promoter.

(A) *HY5* expression as measured by RT-qPCR in wild-type, *srs5-2*, and estradiol-treated *SRS5ox* seedlings grown under white light. Expression levels were normalized against that in wild-type seedlings, which was set to 1. Data are means ± SD of three independent biological replicates. Asterisks indicate significant difference at ***P < 0.001 (Student's *t* test; Supplemental File 1).

(B) Immunodetection of HY5 in wild type, *srs5-2*, and estradiol-treated *SRS5ox* seedlings grown under white light (top). Relative HY5 band intensities of the immunoblot analysis (bottom panel). HY5 protein level in wild-type seedlings was set to 1. The error bars indicate the SD from triplicate experiments. Asterisks indicate significant difference at ***P < 0.001 (Student's *t* test; Supplemental File 1).

(C) Nuclear localization of SRS5-GFP. The wild-type and *Pro35S:SRS5-GFP* seedlings were stained with propidium iodide. Fluorescence microscopy images show SRS5-GFP fusion protein in the nucleus in *Pro35S:SRS5-GFP* plants. Bar = 20 μm.

(D) Schematic diagram of the DNA fragments used for ChIP and the probes used for EMSA. The sequences 1 kb upstream of the start sites and parts of the coding sequences of *HY5* are shown. The translational start site (ATG) is shown at position +1.

(E) Enrichment of the indicated DNA fragments following ChIP using anti-SRS5 antibodies. Chromatin from estradiol-treated or nontreated *SRS5ox* plants was immunoprecipitated using anti-SRS5 antibodies, and the presence of the indicated DNA in the immune complex was determined by RT-qPCR. The numbers of the analyzed DNA fragments indicate the positions relative to the translation start site (referred to as position +1). The *ACTIN7* promoter fragment was used as a negative control. The ChIP values were normalized to their respective DNA inputs. The experiments were repeated three times with similar results. Data shown are representative of three independent experiments. Error bars indicate SE of three technical replicates.

(F) EMSA of SRS5 binding to *HY5 in vitro*. Biotin-labeled probes were incubated with SRS5, and free and bound DNAs were separated in an acrylamide gel. As indicated, unlabeled probes were used as competitors.

this promoter element could be the SRS5 target. This hypothesis was supported by the finding that a similar unlabeled DNA probe with a mutated element in the consensus sequence (mCompetitor) did not affect the binding of SRS5 to the P1 region of the *HY5* promoter (Figure 3F). Together, these results indicate that SRS5 regulates *HY5* expression via direct association with its promoter.

Finally, we tested whether a mutation in *HY5* can rescue the *SRS5ox* phenotype. For this, a *SRS5ox hy5* line was obtained by crossing. Our data showed that the short-hypocotyl phenotype of *SRS5ox* seedlings was partially reversed in *SRS5ox hy5* seedlings grown in either the light or the dark in the presence of estradiol (Figure 4). Thus, combined with the above data that SRS5 stimulates *HY5* expression, these results indicate that
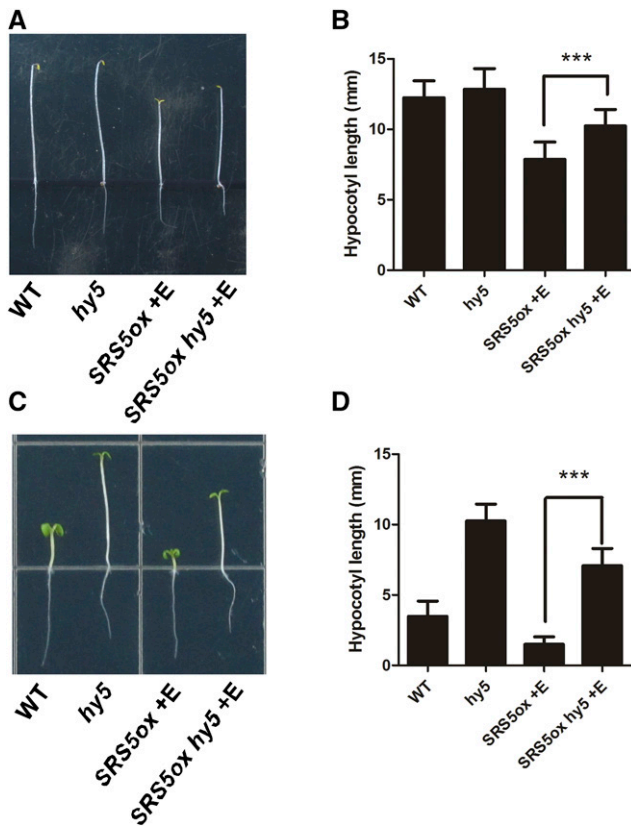
Figure 4. The Short Hypocotyl of *SRS5ox* Seedlings Is Partially Rescued by *hy5*.

(A) and **(C)** Five-day-old Arabidopsis seedlings grown in the dark **(A)** or in blue light (14.9 μmol m^{-2} s^{-1}) **(C)**.

(B) and **(D)** Hypocotyl lengths of wild-type, *hy5*, estradiol-treated *SRS5ox*, and estradiol-treated *hy5 SRS5ox* seedlings grown in the dark **(B)** or in blue light (14.9 μmol m^{-2} s^{-1}) **(D)**.

Data are means ± SD; $n \geq 30$. Asterisks indicate significant differences between *SRS5ox* and *hy5 SRS5ox* (Student's *t* test; Supplemental File 1). ***P < 0.001.

SRS5 promotes photomorphogenesis via direct modulation of *HY5* expression.

SRS5 Degradation Mediated by COP1 Ensures Proper Seedling Development

Since posttranslational regulation plays essential roles in the accumulation of several transcriptional factors that are involved in photomorphogenesis, including HY5, BBX21, and BBX22 (Holm et al., 2002; Datta et al., 2008; Chang et al., 2011; Xu et al., 2016), we assessed the effect of posttranslational regulation on SRS5 accumulation. We found that SRS5 accumulation in estradiol-treated *SRS5ox* seedlings significantly decreased following a transition from the light to the dark in spite of similar *SRS5* transcript levels observed in seedlings either maintained in the light or moved to the dark (Figures 5A and 5B). Also, SRS5 accumulation in various fluence rates of different light

was examined. We found that the levels of SRS5 proteins were higher in *SRS5ox* seedlings exposed to blue, red, and far-red light, compared with in continuous dark (Supplemental Figure 4). These results indicate that posttranslational regulation affects SRS5 abundance.

COP1 functions as a central repressor of seedling photomorphogenesis and ubiquitinates a number of targets, including HY5 and BBX21, promoting their degradation in the dark. Therefore, we hypothesized that COP1 also plays a role in the posttranslational regulation of SRS5. Protein interaction assays using the yeast two-hybrid system showed that SRS5 can physically interact with COP1 (Figure 5C). This COP1-SRS5 protein interaction was further verified via bimolecular fluorescence complementation (BiFC) by transient expression of *SRS5-nYFP* and *COP1-cYFP* in *Nicotiana benthamiana* leaves. In contrast to the lack of YFP fluorescence in the negative control, *N. benthamiana* leaf epidermal cells coexpressing *SRS5-nYFP* and *COP1-cYFP* displayed a reconstituted YFP signal (Figure 5D), indicating that SRS5 directly interacts with COP1. In addition, coimmunoprecipitation (co-IP) assays revealed that COP1 was pulled down using anti-GFP in *Pro35S:SRS5-GFP* seedlings, whereas no COP1 signal resulted from the same co-IP in wild-type seedlings, demonstrating that SRS5 associates with COP1 in vivo (Figure 5E). Furthermore, the involvement of the 26S proteasome in SRS5 degradation was verified by our observation that treatment with MG132, a 26S proteasome inhibitor, resulted in the increased accumulation of SRS5 proteins in *SRS5ox* grown in the dark (Figure 5F). While SRS5 accumulation in estradiol-treated *SRS5ox* seedlings significantly decreased, SRS5 accumulation in estradiol-treated *SRS5ox cop1-4* seedlings was maintained following a transition from the light to the dark (Figure 5A). Consistent with this, after transfer to the dark, SRS5 accumulation was significantly decreased in wild-type seedlings, but SRS5 accumulation was unchanged in *cop1-4* seedlings (Supplemental Figure 5). These data demonstrated that COP1 promotes SRS5 degradation.

We further tested whether COP1 is able to ubiquitinate SRS5 with in vitro ubiquitination assays. The full-length COP1 with an N-terminal MBP tag was expressed and purified in *E. coli*, and its self-ubiquitination activity was tested by incubation with E1 (UBE1), E2(UbcH5b), and myc-tagged ubiquitin (Figure 5G). While in the absence of E1 or E2, no polyubiquitination conjugates was observed, polyubiquitinated MBP-COP1 conjugates were observed when all reagents were present (Figure 5G). When SRS5 was added together with MBP-COP1 in the reaction, both ubiquitinated SRS5 and MBP-COP1 were detected (Figure 5G). However, when MBP was added together with SRS5, no polyubiquitination conjugates were observed. Taken together, these results reveal that COP1 is able to ubiquitinate SRS5 in vitro.

Lastly, we explored whether the role of COP1 in photomorphogenesis includes promoting SRS5 degradation. Whereas SRS5 was less abundant in *SRS5ox 35S:COP1* than in *SRS5ox* plants, we observed higher SRS5 accumulation in *SRS5ox cop1-4* compared with that in *SRS5ox* (Figure 6A). Our assays also showed that *SRS5ox cop1-4* had more SRS5 protein than *cop1-4*, and *cop1-4* accumulated more SRS5 protein than the wild type (Supplemental Figure 6). Together, these data indicated that COP1 promotes the selective degradation of SRS5. Subsequent
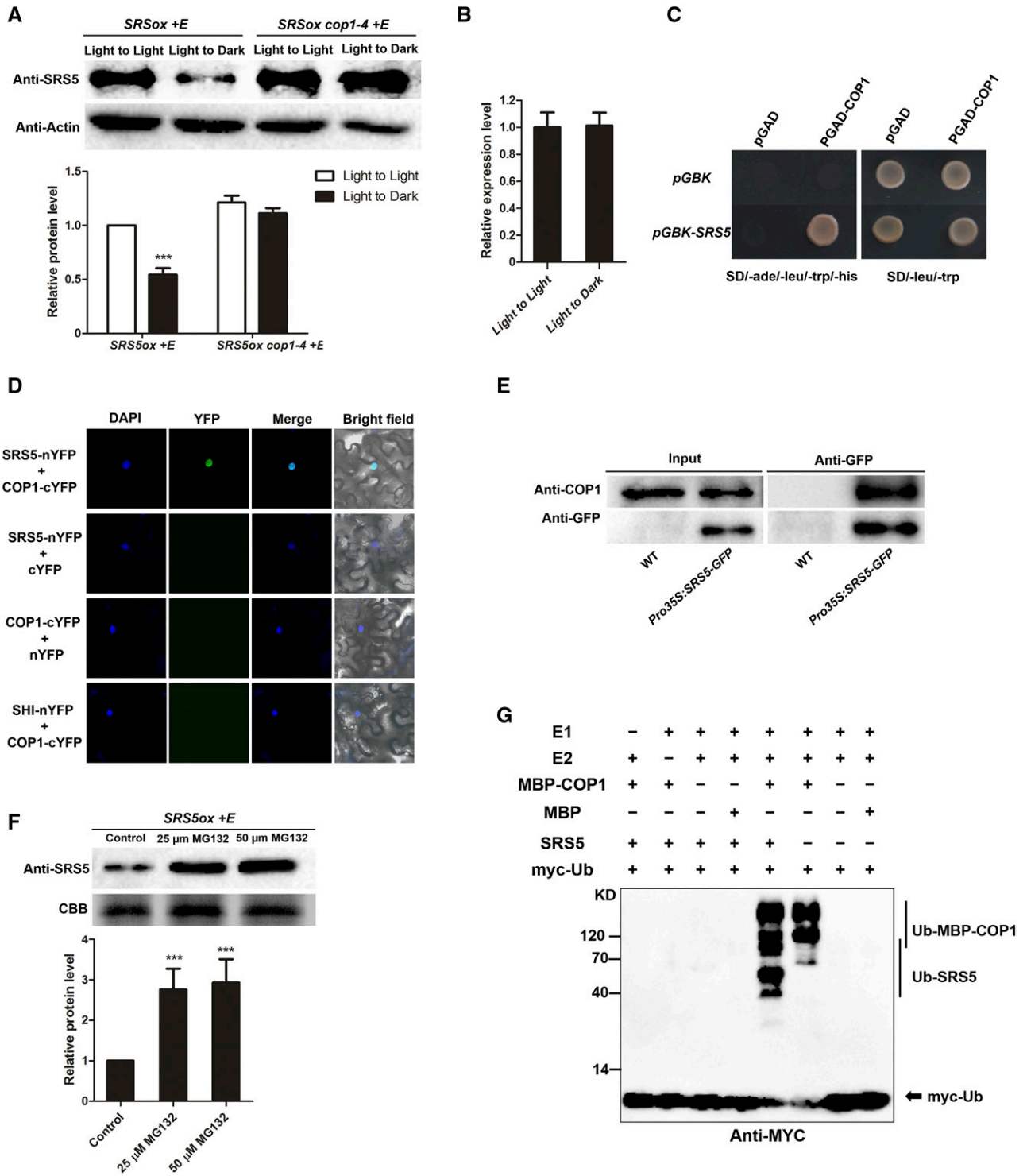
Figure 5. SRS5 Abundance Is Controlled by COP1-Mediated Degradation.

(A) Immunodetection of SRS5 in estradiol-treated *SRS5ox* and *SRS5ox cop1-4* seedlings which were grown under white light for 5 d and then transferred to darkness for 12 h compared with that in the seedlings under continuous white light (top). Anti-actin served as a loading control. Relative SRS5 band intensities of the immunoblot analysis (bottom panel). SRS5 protein level in estradiol-treated *SRS5ox* under continuous light was set to 1. The error bars indicate the SD from triplicate experiments. Asterisks indicate significant difference at ***P < 0.001 (Student's *t* test; Supplemental File 1).
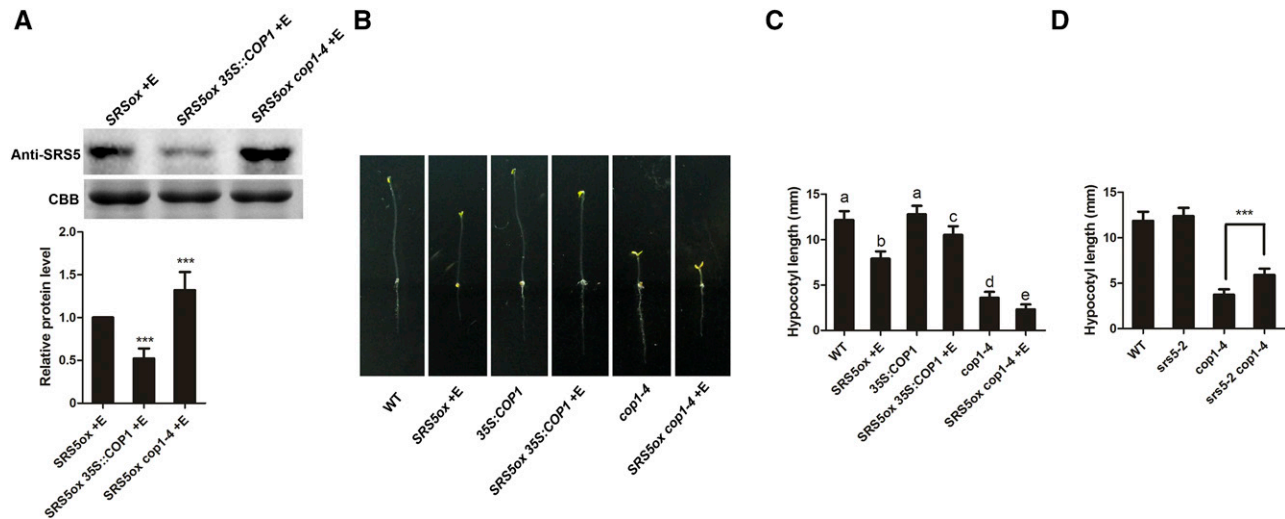
Figure 6. COP1 Controls SRS5 Abundance in Plant Photomorphogenesis.

(A) Immunodetection of SRS5 in estradiol-treated *SRS5ox*, *35S:COP1 SRS5ox* and *cop1-4 SRS5ox* grown in darkness (top). Relative SRS5 band intensities of the immunoblot analysis (bottom panel). SRS5 protein level in estradiol-treated *SRS5ox* was set to 1. The error bars indicate the SD from triplicate experiments. Asterisks indicate significant difference at ***P < 0.001 (Student's *t* test; Supplemental File 1).

(B) The dark-grown phenotypes of 5-d-old seedlings of the wild type, estradiol-treated *SRS5ox*, *35S:COP1*, estradiol-treated *SRS5ox 35S:COP1*, *cop1-4*, and estradiol-treated *SRS5ox cop1-4*.

(C) Quantitation of hypocotyl lengths in seedlings from **(B)**. Data are means ± SD; *n* ≥ 30. Different letters indicate significant differences between the annotated columns (P < 0.05 by Tukey's test).

(D) Hypocotyl lengths of wild-type, *srs5-2*, *cop1-4*, and *srs5-2 cop1-4* seedlings grown in the dark. Data are means ± SD; *n* ≥ 30. Asterisks indicate significant differences between *cop1-4* and *srs5-2 cop1-4* (Student's *t* test; Supplemental File 1). ***P < 0.001.

examination of *SRS5ox 35S:COP1* and *SRS5ox cop1-4* plant phenotypes in the dark showed that estradiol-treated *SRS5ox 35S:COP1* had shorter hypocotyls than *35S:COP1* seedlings (Figures 6B and 6C). Likewise, the constitutive photomorphogenesis phenotype of *cop1-4* seedlings was more severe when accompanied by *SRS5* overexpression in *SRS5ox cop1-4* (Figures 6B and 6C). These phenotypes are consistent with the observed SRS5 accumulation in *SRS5ox 35S:COP1* and *SRS5ox cop1-4* seedlings described above. Furthermore, we generated *srs5-2 cop1-4* plants by crossing *srs5-2* with *cop1-4* and found that the *srs5-2 cop1-4* double mutant had longer hypocotyls than the *cop1-4* mutant in the dark (Figure 6D). These

results support the hypothesis that COP1-mediated degradation of SRS5 is essential for COP1 repression of seedling photomorphogenesis.

SRS5 Directly Activates Expression of the Photomorphogenesis-Promoting Factors *BBX21* and *BBX22*

BBX proteins, including BBX21 and BBX22, positively regulate photomorphogenesis in the light and undergo COP1-mediated degradation in the dark, similar to HY5 (Datta et al., 2008; Chang et al., 2011). Thus, we tested whether SRS5 modulates

---

Figure 5. (continued).

(B) *SRS5* expression assayed by RT-qPCR in estradiol-treated *SRS5ox* after dark treatment for 12 h compared with that in seedlings under continuous light. Expression levels were normalized against that in seedlings under continuous light, which was set to 1. Data are means ± SD of three independent biological replicates.

(C) Yeast two-hybrid interaction assay showing the interaction of SRS5 and COP1.

(D) BiFC assay showing the interaction of SRS5 and COP1 in *N. benthamiana* leaves. Coexpressing *SHI-nYFP* and *COP1-cYFP* and unfused YFP C-terminal (cYFP) or N -terminal (nYFP) fragments served as negative controls, as indicated. DAPI staining marked nuclei. Merge: Merged images of YFP channel and DAPI.

(E) Co-IP analysis showing that SRS5 interacts with COP1 in vivo. Wild-type and *Pro35S:SRS5-GFP* seedlings were used in a co-IP assay using anti-GFP antibodies, and the immunoprecipitated proteins were analyzed by immunoblot using anti-COP1 and anti-GFP, respectively.

(F) Immunodetection of SRS5 abundance in estradiol-treated *SRS5ox* seedlings in the presence of various concentrations of MG132 (25 or 50 μM) for 3 h (top). Relative SRS5 band intensities of the immunoblot analysis (bottom panel). SRS5 protein level in estradiol-treated *SRS5ox* without MG132 treatment was set to 1. The error bars indicate the SD from triplicate experiments. Asterisks indicate significant difference at ***P < 0.001 (Student's *t* test; Supplemental File 1).

(G) COP1 ubiquitinates SRS5 in vitro. In vitro ubiquitination assays were performed in a reaction mix containing UBE1 (E1), UbcH5b (E2), and myc-tagged ubiquitin (myc-Ub). Ubiquitinated MBP-COP1 and SRS5 were detected by anti-myc. The "+" and "−" indicate presence and absence, respectively.

expression of *BBX21* and *BBX22* in addition to *HY5*. We found that the transcripts of *BBX21* and *BBX22* were upregulated in estradiol-treated *SRS5ox* but reduced in *srs5-2* compared with that in the wild type (Figures 7A and 7C).

As a transcription factor, SRS5 may modulate the expression of *BBX21* and *BBX22* by binding to their promoter sequences, as was demonstrated for *HY5*. In support of this notion, the AATCTAC sequence was identified once in the *BBX21* promoter (−1934 to −1941 bp) and the ATTCTAC sequence was identified twice in the *BBX22* promoter (−687 to −694 bp and −677 to −684 bp). These sequences are similar to the consensus sequence ACTCTAC (Eklund et al., 2010). Furthermore, ChIP-qPCR assays indicated that *BX21* and *BBX22* promoter regions were strongly enriched in anti-SRS5 immunoprecipitated chromatin from estradiol-treated *SRS5ox* plants compared with that from nontreated *SRS5ox* plants (Figures 7B and 7D). These results indicate that SRS5 directly activates *BBX21/22* expression by directly binding to their promoters, which underlies the function of SRS5 in photomorphogenesis.

Previous reports have shown that HY5, BBX21, and BBX22 can modulate the expression of many downstream genes involved in plant photomorphogenesis (Lee et al., 2007; Shin et al., 2007;

Chang et al., 2011; Jing et al., 2013). Therefore, we explored whether SRS5 regulates the expression of genes affected by the activity of HY5 or BBX21 and BBX22. RNA sequencing data revealed that many genes related to photomorphogenesis, including hypocotyl cell elongation-related and flavonoid/anthocyanin biosynthetic genes, were affected in estradiol-treated *SRS5ox* plants (Figure 8A; Supplemental Data Set 1). For example, in these *SRS5* overexpression plants, the expression of hypocotyl cell elongation-related genes such as *IAA19*, *XTR6*, *EXT3*, and *EXP3* was downregulated and the expression of genes involved in flavonoid/anthocyanin biosynthesis such as *CHS*, *CHI*, *F3H*, *F2H*, *FLS*, *MYB4*, and *MYB12* was upregulated (Figure 8A). Furthermore, we verified the expression of several genes among them by RT-qPCR and indicated that while *IAA19*, *XTR6*, and *EXT3* were downregulated in estradiol-treated *SRS5ox* but upregulated in *srs5-2* compared with that in the wild type (Figures 8B to 8D), the transcripts level of *CHS*, *CHI*, and *F3H* was higher in estradiol-treated *SRS5ox* but lower in *srs5-2* than in the wild type (Figures 8E to 8G). These expression changes are reminiscent of those induced by HY5 or BBX21 and BBX22 activity (Lee et al., 2007; Shin et al., 2007; Chang et al., 2011; Jing et al., 2013). Therefore, these data further support the idea that SRS5
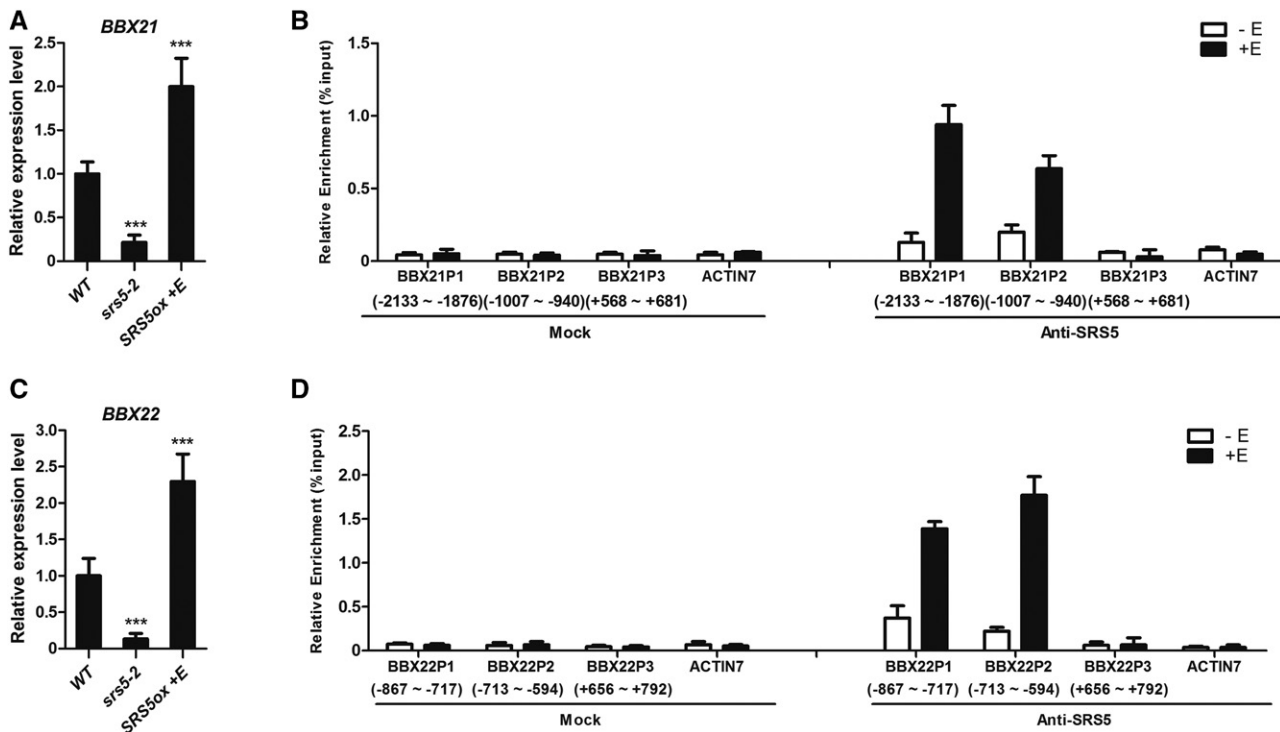
Figure 7. SRS5 Activates Photomorphogenesis-Promoting Genes *BBX21* and *BBX22* by Directly Binding to Their Promoters.

(A) and **(C)** The expression levels of *BBX21* **(A)** and *BBX22* **(C)** in wild-type, *srs5-2*, and estradiol-treated *SRS5ox* seedlings grown under white light were assayed by RT-qPCR. Expression levels were normalized against that in wild-type seedlings, which was set to 1. Data are means ± sp of three independent biological replicates. Asterisks indicate significant difference at ***P < 0.001 (Student's *t* test; Supplemental File 1).

(B) and **(D)** ChIP-qPCR was performed for the *BBX21* **(B)** and *BBX22* **(D)** promoters. The numbers of the analyzed DNA fragments indicate the positions relative to the translation start site (referred to as position +1). The *ACTIN7* promoter fragment was used as a negative control. The ChIP values were normalized to their respective DNA inputs. The experiments were repeated three times with similar results. Data shown are representative of three independent experiments. Error bars represent sɛ of three technical replicates.

A

ANNOTATION	GENE MODEL	Ratio	P_value	FDR
Hypocotyl cell elongation-related genes				
IAA19	AT3G15540.1	0.49	2.3E-13	5.6E-13
EXT3	AT1G21310.1	0.46	0	0
EXT4	AT1G76930.1	0.36	2.3E-09	4.3E-09
XTR4	AT2G06850.1	0.07	9.9E-11	2.0E-10
XTR6	AT4G25810.1	0.11	8.4E-11	1.7E-10
XTR22	AT5G57560.1	0.38	1.7E-15	4.9E-15
EXPA1	AT1G69530.3	0.48	6.3E-12	1.4E-11
EXPA4	AT2G39700.1	0.21	0	0
EXPA6	AT2G28950.1	0.26	0	0
Flavonoid and anthocyanin biosynthesis pathways				
CHS	AT5G13930.1	3.07	0	0
CHI	AT3G55120.1	3.78	0	0
MYB4	AT4G38620.1	3.64	0	0
MYB12	AT2G47460.1	2.61	1.2E-17	3.6E-17
F2H	AT1G05055.1	2.28	1.5E-37	5.0E-37
F3H	AT3G51240.1	2.84	2.2E-14	9.0E-14
FLS	AT5G08640.1	2.30	7.4E-87	2.9E-86

Figure 8. Genes Related to Photomorphogenesis Differentially Regulated in Estradiol-Treated *SRS5ox* Plants.

(A) The expression levels of genes related to photomorphogenesis assayed by RNA-seq in 5-d-old *SRS5ox* seedlings grown under white light treated with or without estradiol for 2 h, respectively. The expression ratios were calculated using the formula: ratio = *SRS5ox* +E/ *SRS5ox* –E. FDR, false discovery rate.

(B) to **(G)** The expression levels of *IAA19* **(B)**, *XTR6* **(C)**, *EXT3* **(D)**, *CHS* **(E)**, *CHI* **(F)**, and *F3H* **(G)** in wild-type, *srs5-2*, and estradiol-treated *SRS5ox* seedlings grown under white light were assayed by RT-qPCR. Expression levels were normalized against that in wild-type seedlings, which was set to 1. Data are means ± SD of three independent biological replicates. Asterisks indicate significant difference at ***P < 0.001 (Student's *t* test; Supplemental File 1).

modulates plant photomorphogenesis by regulating the expression of other photomorphogenesis-promoting genes including *HY5*, *BBX21*, and *BBX22.*

DISCUSSION

Light is one of the most influential environmental signals that affect plant development. The activation of different photoreceptors by varying light qualities modulates core signaling networks and induces several plant photomorphogenesis-promoting factors, including HY5, BBX21, and BBX22 (Jiao et al., 2007; Gangappa and Botto, 2014). In this study, we identified the transcription factor SRS5 as a positive player in signaling that promotes photomorphogenesis. This role for SRS5 is exemplified by longer hypocotyl phenotype of light-grown *srs5-2* seedlings compared with that of the wild type. Whereas overexpression of other well-known photomorphogenesis-promoting factors such as HY5, BBX21, and BBX22 does not result in photomorphogenesis in dark-grown seedlings (Ang et al., 1998; Holm et al., 2002; Chang et al., 2011; Xu et al., 2016), *SRS5* overexpression leads to constitutive photomorphogenesis that is characterized by shorter hypocotyls and more open cotyledons compared

with those in wild-type seedlings grown in the dark. This *SRS5* overexpression phenotype is likely due to SRS5 binding to promoter regions and upregulating the expression of the photomorphogenesis-promoting genes *HY5*, *BBX21*, and *BBX22*. Thus, SRS5 acts as a positive regulator of photomorphogenesis that upregulates the expression of photomorphogenesis-promoting genes to modulate plant light responses.

While HY5, BBX21, and BBX22 play key roles in light signaling, SRS5 also functions in photomorphogenesis by modulating the expression of *HY5*, but the short-hypocotyl phenotype of *SRS5ox* seedlings is partially reversed in *SRS5ox hy5* seedlings grown in either the light or the dark in the presence of estradiol, implying that besides *HY5*, other factors may be also involved in *SRS5*-promoted photomorphogenesis. Indeed, SRS5 also binds to the promoters of *BBX21* and *BBX22* to activate their expression. In addition, our ChIP-qPCR assays showed that the promoter regions of both *CHS* and *CHI* genes were enriched in anti-SRS5 immunoprecipitated chromatin from estradiol-treated *SRS5ox* plants compared with that from untreated control (Supplemental Figure 7), suggesting that SRS5 could bind to *CHS* and *CHI* promoters to modulate their expression.

SRS5 is a member of the *SHI* gene family, which is characterized by the presence of two functional domains: a 43-amino acid RING-like zinc finger domain and a more C-terminal, unique IGGH domain (Kuusk et al., 2002; Eklund et al., 2010). This RING-like zinc finger domain consists of two fingers that may form a cross-brace arrangement, resembling a DNA binding domain. The IGGH domain carries several acidic residues is involved in mediating the homo- and heterodimerization between SHI family proteins (Fridborg et al., 2001; Eklund et al., 2010). STY1, a member of the *SHI* family, directly binds to the *YUCCA4* promoter to regulate auxin biosynthesis (Eklund et al., 2010). Several family members regulate leaf vein development in Arabidopsis, which is related to their functions in auxin biosynthesis (Baylis et al., 2013). To further explore the potential function of other *SHI* family genes in photomorphogenesis, we examined the phenotypes of loss-of-function mutants of *SHI* family genes *SHI*, *SHI-RELATED SEQUENCE7* (*SRS7*), and *LATERAL ROOT PRIMORDIUM1* (*LRP1*) and found that these mutants have similar hypocotyl length as the wild type grown either in the light or in darkness. We also obtained double mutants *srs5-2 shi*, *srs5-2 srs7*, and *srs5-2 lrp1* by crossing *srs5-2* with *shi*, *srs7*, and *lrp1*, respectively. The hypocotyl lengths of these double mutants were comparable to those of *srs5-2* seedlings grown either in the light or in darkness (Supplemental Figure 8).

COP1, a central player in light signaling pathways, represses photomorphogenesis in dark-grown seedlings by ubiquitinating photomorphogenesis-promoting factors, including HY5, BBX21, and BBX22, thus promoting their degradation (Osterlund et al., 2000b; Wang et al., 2001; Lau and Deng, 2010). Our results revealed that SRS5 physically interacts with COP1 and that SRS5 accumulation is reduced following *COP1* overexpression, whereas SRS5 accumulation is further increased in the *cop1-4* mutant, which lacks COP1 function. Furthermore, *SRS5* overexpression enhanced the *cop1-4* constitutively photomorphogenic phenotype in dark-grown seedlings, and the short hypocotyl phenotype that accompanied *SRS5* overexpression was reversed by *COP1* overexpression. Therefore, comparable to other photomorphogenesis-promoting factors, such as HY5, BBX21, and BBX22, COP1-mediated SRS5 degradation is also involved in seedling photomorphogenesis.

In conclusion, our study demonstrates that SRS5 acts as a positive regulator of photomorphogenesis. Whereas SRS5 degradation mediated by COP1 is essential for skotomorphogenesis in the dark, increased *SRS5* expression in the light leads to the positive modulation of photomorphogenesis via SRS5-mediated activation of other photomorphogenesis-promoting genes through direct binding of their promoters (Figure 9).

METHODS

Plant Materials

The *Arabidopsis thaliana* lines *srs5-2* (Salk_019951), *hy5* (SALK_096651), *cry1* (SALK_069292), *srs7* (salk_151552), *shi* (N126329), and *lrp1* (SAIL_70_H09) were obtained from the ABRC (http://www.arabidopsis.org/abrc). All of the mutant lines used in this study were verified by PCR and RT-PCR. Double mutant lines were obtained by crossing and were
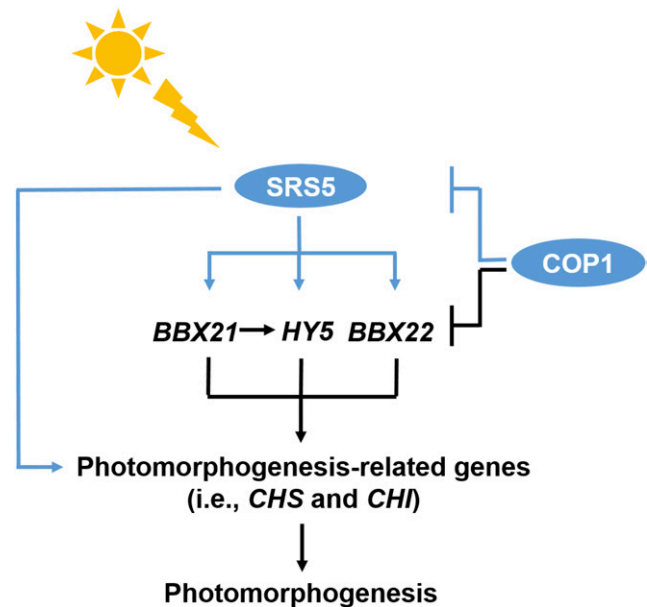
Figure 9. Model for the Role of SRS5 in Photomorphogenesis.

Blue light-induced SRS5 promotes seedling photomorphogenesis by directly activating several other photomorphogenesis-promoting genes such as *HY5*, *BBX21*, and *BBX22*, but COP1 directly targets SRS5 for 26S proteasome-mediated degradation in the dark.

confirmed by PCR. All PCR primers used for genotyping are listed in Supplemental Table 1. The published transgenic lines used in this study are *cop1-4* (Saijo et al., 2003), *35S:COP1* (Wang et al., 2001), and *cry1 cry2* (Mao et al., 2005).

Plant Growth

Arabidopsis seeds were surface sterilized with 5% (w/v) bleach for 5 min, washed three times with sterile water, placed at 4°C for 3 d, and then planted on medium containing 0.5× MS, 1% sucrose, and 1% (m/v) agar at pH 5.8 (adjusted using 1 M KOH). Seedlings were grown at 23°C under a long-day photoperiod (16-h white light [100 µmol m^{-2} s^{-1}]/8-h dark), under blue light (14.9 µmol m^{-2} s^{-1}), under red light (25.3 µmol m^{-2} s^{-1}), under far-red light (41.7 µmol m^{-2} s^{-1}), or in darkness for 5 d. The biotron (model LH-100SP-LED; NK Systems) with LED lighting unit was used. Blue, red, and far-red light were generated at 470, 655, and 730 nm, respectively. For estradiol treatment, β-estradiol (Sigma-Aldrich) was added to the culture medium where indicated.

Genetic Screen

To screen for mutants that exhibit photomorphogenesis in the dark, Arabidopsis T-DNA insertion lines were generated with an estradiol-inducible expression system driven by the chimeric transcription activator XVE (Zuo et al., 2000). Over 12,000 XVE tagging T-DNA insertion lines were obtained and the seeds per each line were harvested individually. Then, 20 seeds of one independent line were planted on the medium with 5 µM estradiol and grown in the dark. The seedlings after their growth for 1 week were examined for phenotypic analysis, and a mutant *SRS5ox* was obtained as it exhibits short hypocotyl and open cotyledons compared with wild-type seedlings. The genomic sequence surrounding the

XVE T-DNA in *SRS5ox* was identified by thermal asymmetric interlaced PCR (Liu et al., 1995).

Transgene Construction

Agrobacterium tumefaciens (strain C58C1) containing plasmid constructs was used to transform plants by the floral-dip method (Wang et al., 2013). The full-length *SRS5* cDNA was amplified using *SRS5*-forward and *SRS5*-reverse primers and cloned into the *Bam*HI site of pBI121-GFP vector (Yuan et al., 2014) where expression was driven by the CaMV 35S promoter, and then the resulting *Pro35S:SRS5-GFP* plasmid was transformed into Col-0 and *srs5-2* plants.

To construct the *ProSRS5:GUS* plasmid, a 6-kb fragment upstream of the ATG translation initiation codon of *SRS5* was amplified using primers *SRS5* pro-Forward and pro-Reverse and then cloned into the *Sal*I site of pBI101 vector to create the *SRS5:GUS* fusion.

GUS Staining

GUS staining was performed according to methods described previously (Li et al., 2015). Briefly, seedlings were incubated at 37°C in staining solution (100 mM sodium phosphate buffer, pH 7.5, containing 10.0 mM EDTA, pH 8.0, 0.5 mM $K_3[Fe(CN)_6]$, 0.5 mM $K_4[Fe(CN)_6]$, 0.1% Triton X-100, and 1.0 mM 5-bromo-chloro-3-indolyl-β-D-glucuronide). Images of seedlings were acquired using a Nikon camera (DXM1200F) coupled to a stereomicroscope (Olympus SZX12). Biological triplicates, involving three sets of plant grown at separate times, were included for each treatment.

RNA Extraction and RT-qPCR Analysis

Total RNA was isolated from whole seedlings using TRIzol reagent (Invitrogen) as previously described (Zhang et al., 2013). Following treatment with RQ1 RNase-free DNase I (Promega), first-strand cDNA synthesis was performed using Superscript II reverse transcriptase (Invitrogen) according to the manufacturer's instructions. The RT-qPCR analysis was performed using a Bio-Rad CFX96 (Bio-Rad) and SYBR Green I (Invitrogen). PCR was performed in 96-well plates according to the following protocol: 3 min at 95°C followed by 40 cycles of 15 s denaturation at 95°C, 15 s annealing at 58°C, and 20 s extension at 72°C. *ACTIN2* (AT3G18780) and *EIF4A* (AT3G13920) were used as internal controls. All experiments were performed with three independent biological replicates using RNA samples extracted from three independent plant materials grown under identical conditions and three technical repetitions. The primers used for RT-qPCR analysis are listed in Supplemental Table 1.

Immunoblot Analysis

Protein immunoblot analyses were conducted as described previously (Gendrel et al., 2005). Briefly, total protein was extracted from Arabidopsis seedlings, separated by SDS-PAGE, and then electroblotted onto a polyvinylidene difluoride membrane. Membranes were incubated with indicated primary antibodies separately and then incubated with goat anti-rabbit or goat anti-mouse IgG peroxidase conjugate (Sigma-Aldrich) as the secondary antibody. Coomassie Brilliant Blue staining indicates equal total protein loading. When the SRS5 protein level was detected in estradiol-treated *SRS5ox* seedlings after dark treatment, the antibody anti-actin (M20009; Abmart) was used as a loading control. The photographs shown are representative results of three independent assays. The intensity of each band was measured with an image processing and analysis software package (ImageJ). The ratio was calculated by normalizing the intensity of each band to the intensity of the input.

For the detection of HY5 and SRS5 proteins, the antibody anti-HY5 (R1245; Abiocode) and antibody anti-SRS5 (diluted in 0.02 M PBS, pH 7.4, and 0.01% NaN_3) were used, respectively. To prepare antibody anti-SRS5, full-length recombinant Arabidopsis SRS5 was expressed and purified using *Escherichia coli* and then the purified protein was used to generate a polyclonal anti-SRS5 antibody in the rabbit as previously described (Gendrel et al., 2005). The specificity of anti-SRS5 was tested in Arabidopsis by immunoblot analysis. SRS5 protein was detected in the wild type but not in *srs5-2* mutant seedlings. Besides, the significant increase in SRS5 abundance was observed in estradiol-treated *SRS5ox* seedlings (Supplemental Figure 3).

ChIP

According to a previously described method (Gendrel et al., 2005), 7-d-old estradiol-treated and nontreated *SRS5ox* seedlings grown under white light were fixed at room temperature in 1% formaldehyde under vacuum for 15 min. Fixed tissues were homogenized, and the chromatin was isolated and sonicated. The anti-SRS5 antibody was used for immunoprecipitation. About 5% of nonimmunoprecipitated sonicated chromatin was reverse cross-linked and used as an input DNA control. The immunoprecipitated DNA was recovered and analyzed by RT-qPCR in triplicate replicates with *ACTIN7* (AT5G09810) as negative control. qPCR data were analyzed according to the percentage of input method (Haring et al., 2007; Binkert et al., 2014). All experiments were performed with three independent biological replicates using chromatin samples from three independent plant materials grown under identical conditions. The experiments were repeated three times with similar results. Data shown are representative of three independent experiments. All primers used in the ChIP assays are listed in Supplemental Table 1.

EMSA

The full-length *SRS5* cDNA sequence was cloned in the *pET28a* vector and introduced into the *E. coli* strain BL21 (Invitrogen) to produce SRS5. Purified SRS5 was used for EMSA. Oligonucleotide probes were synthesized and labeled with biotin at their 3′-ends (Invitrogen). EMSA was performed using a Light Shift Chemiluminescent EMSA kit (Thermo Scientific). Briefly, biotin-labeled probes were incubated in 1× binding buffer, 2.5% glycerol, 50 mM KCl, 5 mM $MgCl_2$, and 10 mM EDTA with or without proteins at room temperature for 20 min. For competition experiments, nonlabeled probes were added to the binding reactions. The probe sequences are listed in Supplemental Table 2.

Yeast Two-Hybrid Assays

To verify the interaction between SRS5 and COP1 in yeast, the coding sequence (CDS) of *SRS5* was fused to the DNA binding domain (BD) in pGBKT7, and the CDSs of *COP1* were individually cloned into the pGADT7. The interactions between proteins were assayed by the mating method as described (Clontech Laboratories; Matchmaker GAL4 Two-Hybrid System and Libraries User Manual) (Yuan et al., 2017).

BiFC Assays

For the BiFC assays, the CDS of Arabidopsis *SRS5* was cloned into *pUC-YNE* (containing the YFP N terminus), and the CDS of *COP1* was cloned into *pUC-YCE* (containing the YFP C terminus) (Walter et al., 2004). The sequences of the primers used to generate these constructs are listed in Supplemental Table 1. Constructs for the expression of *SRS5-nYFP* and *COP1-cYFP* were introduced into *Nicotiana benthamiana* leaves via agroinfiltration. After 2 d of incubation, YFP fluorescence was observed

in transformed leaf epidermal cells using a laser confocal microscope (Olympus FluoView 1000-Confocal laser scanning microscope).

Co-IP Assays

For co-IP assays, total proteins were extracted from 7-d-old *Pro35S: SRS5*-GFP seedlings and immunoprecipitated with anti-GFP (Sigma-Aldrich). The immunoprecipitated proteins were separated by SDS-PAGE and subject to immunoblot analysis using anti-COP1 antibody (Abiocode) and anti-GFP (Sigma-Aldrich).

In Vitro Ubiquitination Assays

The full-length *COP1* cDNA sequence was fused with N-terminal MBP coding region, and MBP-COP1 fusion was cloned into the *pET28a* vector and introduced into the *E. coli* strain BL21 (Invitrogen) to produce MBP-COP1. According to a previously described method (Saijo et al., 2003), ubiquitination reaction mixtures (30 µL) contained 50 ng of UBE1 (E1; Boston Biochem), 200 ng of UbcH5b (E2; Boston Biochem), 5 µg of myc-tagged ubiquitin (myc-Ub; Boston Biochem), 500 ng of SRS5, and 200 ng of MBP-COP1 in a reaction buffer containing 50 mM Tris, pH 7.5, 5 mM $MgCl_2$, 2 mM ATP, and 2 mM DTT. After incubation at 30°C for 2 h, the reactions were stopped with sample loading buffer by boiling at 100°C, separated by SDS-PAGE, and analyzed by immunoblots using antibody monoclonal anti-myc (M4439; Sigma-Aldrich) and antibody anti-SRS5, respectively.

RNA Sequencing

RNA samples were collected from 5-d-old *SRS5ox* seedlings grown under white light treated with or without estradiol for 2 h, respectively. Library construction and sequencing were performed by the Beijing Genomic Institution (Shenzhen, China). Clean tags were mapped to the reference genome and genes available at the ABRC (http://www.arabidopsis.org/abrc). The expression ratios were calculated using the formula: ratio = *SRS5ox* +E/*SRS5ox* −E.

Accession Numbers

The TAIR accession numbers for the sequences used in this study are as follows: *SRS5* (AT1G75520), *HY5* (AT5G11260), *COP1* (AT2G32950), *BBX21* (AT1G75540), *BBX22* (AT1G78600), *SHI* (AT5G66350), *SRS7* (AT1G19790), *LRP1* (AT5G12330), *CHS* (AT5G13930), *CHI* (AT3G55120), *F3H* (AT3G51240), *EXT3* (AT1G21310), *IAA19* (AT3G11540), and *XTR6* (AT4G25810). RNA-seq data are available at the National Center for Biotechnology Information Sequence Read Archive (http://www.ncbi.nlm.nih.gov/sra) under accession number SRP158356.

Supplemental Data

Supplemental Figure 1. Phenotypes of *SRS5ox* and *srs5-2* seedlings under red or far-red light.

Supplemental Figure 2. Expression patterns of *SRS5* in response to red or far-red light.

Supplemental Figure 3. Immunodetection of SRS5 in the wild type, estradiol-treated *SRS5ox*, and *srs5-2*.

Supplemental Figure 4. Light-induced accumulation of SRS5 proteins.

Supplemental Figure 5. Immunodetection of SRS5 in wild-type and *cop1-4* seedling following a transition from the light to the dark.

Supplemental Figure 6. Immunodetection of SRS5 in *cop1-4*, estradiol-treated *cop1-4 SRS5ox*, and wild-type seedlings grown in darkness.

Supplemental Figure 7. SRS5 directly binds to the promoters of *CHS* and *CHI*.

Supplemental Figure 8. Phenotypes of single or double mutants of *SHI* family genes under dark, blue, red, or far-red light.

Supplemental Table 1. List of the primers used in this study.

Supplemental Table 2. List of oligonucleotides used for EMSA.

Supplemental Data Set 1. Raw RNA-seq data for differential expression genes in estradiol-treated *SRS5*ox plants.

Supplemental File 1. Statistical analysis.

AUTHOR CONTRIBUTIONS

T.-T.Y. and Y.-T.L. designed the experiments. T.-T.Y., H.-H.X., Q.Z., and L.-Y.Z. performed the experiments. T.-T.Y. and Y.-T.L. wrote the article.

REFERENCES

Abbas, N., Maurya, J.P., Senapati, D., Gangappa, S.N., and Chattopadhyay, S. (2014). Arabidopsis CAM7 and HY5 physically interact and directly bind to the HY5 promoter to regulate its expression and thereby promote photomorphogenesis. Plant Cell **26:** 1036–1052.

Ang, L.H., Chattopadhyay, S., Wei, N., Oyama, T., Okada, K., Batschauer, A., and Deng, X.W. (1998). Molecular interaction between COP1 and HY5 defines a regulatory switch for light control of Arabidopsis development. Mol. Cell **1:** 213–222.

Baylis, T., Cierlik, I., Sundberg, E., and Mattsson, J. (2013). SHORT INTERNODES/STYLISH genes, regulators of auxin biosynthesis, are involved in leaf vein development in *Arabidopsis thaliana*. New Phytol. **197:** 737–750.

Binkert, M., Kozma-Bognár, L., Terecskei, K., De Veylder, L., Nagy, F., and Ulm, R. (2014). UV-B-responsive association of the Arabidopsis bZIP transcription factor ELONGATED HYPOCOTYL5 with target genes, including its own promoter. Plant Cell **26:** 4200–4213.

Chang, C.S., Maloof, J.N., and Wu, S.H. (2011). COP1-mediated degradation of BBX22/LZF1 optimizes seedling development in Arabidopsis. Plant Physiol. **156:** 228–239.

Chen, M., Chory, J., and Fankhauser, C. (2004). Light signal transduction in higher plants. Annu. Rev. Genet. **38:** 87–117.

Datta, S., Johansson, H., Hettiarachchi, C., Irigoyen, M.L., Desai, M., Rubio, V., and Holm, M. (2008). LZF1/SALT TOLERANCE HOMOLOG3, an Arabidopsis B-box protein involved in light-dependent development and gene expression, undergoes COP1-mediated ubiquitination. Plant Cell **20:** 2324–2338.

Eklund, D.M., Ståldal, V., Valsecchi, I., Cierlik, I., Eriksson, C., Hiratsu, K., Ohme-Takagi, M., Sundström, J.F., Thelander, M., Ezcurra, I., and Sundberg, E. (2010). The *Arabidopsis thaliana* STYLISH1 protein acts as a transcriptional activator regulating auxin biosynthesis. Plant Cell 22: 349–363.

Fridborg, I., Kuusk, S., Moritz, T., and Sundberg, E. (1999). The Arabidopsis dwarf mutant shi exhibits reduced gibberellin responses conferred by overexpression of a new putative zinc finger protein. Plant Cell 11: 1019–1032.

Fridborg, I., Kuusk, S., Robertson, M., and Sundberg, E. (2001). The Arabidopsis protein SHI represses gibberellin responses in Arabidopsis and barley. Plant Physiol. 127: 937–948. 11706176

Gangappa, S.N., and Botto, J.F. (2014). The BBX family of plant transcription factors. Trends Plant Sci. 19: 460–470.

Gendrel, A.V., Lippman, Z., Martienssen, R., and Colot, V. (2005). Profiling histone modification patterns in plants using genomic tiling microarrays. Nat. Methods 2: 213–218.

Haring, M., Offermann, S., Danker, T., Horst, I., Peterhansel, C., and Stam, M. (2007). Chromatin immunoprecipitation: optimization, quantitative analysis and data normalization. Plant Methods 3: 11.

Hoecker, U., and Quail, P.H. (2001). The phytochrome A-specific signaling intermediate SPA1 interacts directly with COP1, a constitutive repressor of light signaling in Arabidopsis. J. Biol. Chem. 276: 38173–38178.

Holm, M., Ma, L.G., Qu, L.J., and Deng, X.W. (2002). Two interacting bZIP proteins are direct targets of COP1-mediated control of light-dependent gene expression in Arabidopsis. Genes Dev. 16: 1247–1259.

Huang, X., Ouyang, X., and Deng, X.W. (2014). Beyond repression of photomorphogenesis: role switching of COP/DET/FUS in light signaling. Curr. Opin. Plant Biol. 21: 96–103.

Jiao, Y., Lau, O.S., and Deng, X.W. (2007). Light-regulated transcriptional networks in higher plants. Nat. Rev. Genet. 8: 217–230.

Jing, Y., Zhang, D., Wang, X., Tang, W., Wang, W., Huai, J., Xu, G., Chen, D., Li, Y., and Lin, R. (2013). Arabidopsis chromatin remodeling factor PICKLE interacts with transcription factor HY5 to regulate hypocotyl cell elongation. Plant Cell 25: 242–256.

Kami, C., Lorrain, S., Hornitschek, P., and Fankhauser, C. (2010). Light-regulated plant growth and development. Curr. Top. Dev. Biol. 91: 29–66.

Kuusk, S., Sohlberg, J.J., Long, J.A., Fridborg, I., and Sundberg, E. (2002). STY1 and STY2 promote the formation of apical tissues during Arabidopsis gynoecium development. Development 129: 4707–4717.

Kuusk, S., Sohlberg, J.J., Magnus Eklund, D., and Sundberg, E. (2006). Functionally redundant SHI family genes regulate Arabidopsis gynoecium development in a dose-dependent manner. Plant J. 47: 99–111.

Lau, O.S., and Deng, X.W. (2010). Plant hormone signaling lightens up: integrators of light and hormones. Curr. Opin. Plant Biol. 13: 571–577.

Lau, O.S., and Deng, X.W. (2012). The photomorphogenic repressors COP1 and DET1: 20 years later. Trends Plant Sci. 17: 584–593.

Lee, J., He, K., Stolc, V., Lee, H., Figueroa, P., Gao, Y., Tongprasit, W., Zhao, H., Lee, I., and Deng, X.W. (2007). Analysis of transcription factor HY5 genomic binding sites revealed its hierarchical role in light regulation of development. Plant Cell 19: 731–749.

Li, J., Xu, H.H., Liu, W.C., Zhang, X.W., and Lu, Y.T. (2015). Ethylene Inhibits Root Elongation during Alkaline Stress through AUXIN1 and Associated Changes in Auxin Accumulation. Plant Physiol. 168: 1777–1791.

Liu, Y.G., Mitsukawa, N., Oosumi, T., and Whittier, R.F. (1995). Efficient isolation and mapping of *Arabidopsis thaliana* T-DNA insert junctions by thermal asymmetric interlaced PCR. Plant J. 8: 457–463.

Ma, L., Li, J., Qu, L., Hager, J., Chen, Z., Zhao, H., and Deng, X.W. (2001). Light control of Arabidopsis development entails coordinated regulation of genome expression and cellular pathways. Plant Cell 13: 2589–2607.

Mao, J., Zhang, Y.C., Sang, Y., Li, Q.H., and Yang, H.Q. (2005). From The Cover: A role for Arabidopsis cryptochromes and COP1 in the regulation of stomatal opening. Proc. Natl. Acad. Sci. USA 102: 12270–12275.

Marsch-Martínez, N., and Pereira, A. (2011). Activation tagging with En/Spm-I /dSpm transposons in Arabidopsis. Methods Mol. Biol. 678: 91–105.

Osterlund, M.T., Hardtke, C.S., Wei, N., and Deng, X.W. (2000b). Targeted destabilization of HY5 during light-regulated development of Arabidopsis. Nature 405: 462–466.

Osterlund, M.T., Wei, N., and Deng, X.W. (2000a). The roles of photoreceptor systems and the COP1-targeted destabilization of HY5 in light control of Arabidopsis seedling development. Plant Physiol. 124: 1520–1524.

Saijo, Y., Sullivan, J.A., Wang, H., Yang, J., Shen, Y., Rubio, V., Ma, L., Hoecker, U., and Deng, X.W. (2003). The COP1-SPA1 interaction defines a critical step in phytochrome A-mediated regulation of HY5 activity. Genes Dev. 17: 2642–2647.

Sang, Y., Li, Q.H., Rubio, V., Zhang, Y.C., Mao, J., Deng, X.W., and Yang, H.Q. (2005). N-terminal domain-mediated homodimerization is required for photoreceptor activity of Arabidopsis CRYPTOCHROME 1. Plant Cell 17: 1569–1584.

Shin, J., Park, E., and Choi, G. (2007). PIF3 regulates anthocyanin biosynthesis in an HY5-dependent manner with both factors directly binding anthocyanin biosynthetic gene promoters in Arabidopsis. Plant J. 49: 981–994.

von Arnim, A.G., and Deng, X.W. (1994). Light inactivation of Arabidopsis photomorphogenic repressor COP1 involves a cell-specific regulation of its nucleocytoplasmic partitioning. Cell 79: 1035–1045.

von Arnim, A.G., Osterlund, M.T., Kwok, S.F., and Deng, X.W. (1997). Genetic and developmental control of nuclear accumulation of COP1, a repressor of photomorphogenesis in Arabidopsis. Plant Physiol. 114: 779–788.

Walter, M., Chaban, C., Schutze, K., Batistic, O., Weckermann, K., Nake, C., Blazevic, D., Grefen, C., Schumacher, K., Oecking, C., Harter, K., and Kudla, J. (2004). Visualization of protein interactions in living plant cells using bimolecular fluorescence complementation. Plant J. 40: 428–438.

Wang, H., Ma, L.G., Li, J.M., Zhao, H.Y., and Deng, X.W. (2001). Direct interaction of Arabidopsis cryptochromes with COP1 in light control development. Science 294: 154–158.

Wang, J., Yan, D.W., Yuan, T.T., Gao, X., and Lu, Y.T. (2013). A gain-of-function mutation in IAA8 alters Arabidopsis floral organ development by change of jasmonic acid level. Plant Mol. Biol. 82: 71–83.

Xu, D., Jiang, Y., Li, J., Lin, F., Holm, M., and Deng, X.W. (2016). BBX21, an Arabidopsis B-box protein, directly activates HY5 and is targeted by COP1 for 26S proteasome-mediated degradation. Proc. Natl. Acad. Sci. USA 113: 7655–7660.

Yang, H.Q., Wu, Y.J., Tang, R.H., Liu, D., Liu, Y., and Cashmore, A.R. (2000). The C termini of Arabidopsis cryptochromes mediate a constitutive light response. Cell 103: 815–827.

Yang, H.Q., Tang, R.H., and Cashmore, A.R. (2001). The signaling mechanism of Arabidopsis CRY1 involves direct interaction with COP1. Plant Cell **13:** 2573–2587.

Yuan, H.M., Liu, W.C., and Lu, Y.T. (2017). CATALASE2 coordinates SA-mediated repression of both auxin accumulation and JA biosynthesis in plant defenses. Cell Host Microbe **21:** 143–155.

Yuan, T.T., Xu, H.H., Zhang, K.X., Guo, T.T., and Lu, Y.T. (2014). Glucose inhibits root meristem growth via ABA INSENSITIVE 5, which represses PIN1 accumulation and auxin activity in Arabidopsis. Plant Cell Environ. **37:** 1338–1350.

Zhang, K.X., Xu, H.H., Yuan, T.T., Zhang, L., and Lu, Y.T. (2013). Blue-light-induced PIN3 polarization for root negative phototropic response in Arabidopsis. Plant J. **76:** 308–321.

Zhang, Y., Zheng, S., Liu, Z., Wang, L., and Bi, Y. (2011). Both HY5 and HYH are necessary regulators for low temperature-induced anthocyanin accumulation in Arabidopsis seedlings. J. Plant Physiol. **168:** 367–374.

Zuo, J., Niu, Q.W., and Chua, N.H. (2000). Technical advance: An estrogen receptor-based transactivator XVE mediates highly inducible gene expression in transgenic plants. Plant J. **24:** 265–273.